Utilizing Spectral Indices to Estimate Total Dissolved Solids in Water Body Northwest Arabian Gulf

Adel Jassim Al-Fartusi[1]*, Mutasim Ibrahim Malik[2], Hameed Majeed Abduljabbar[3]

[1]Physics Department, Marine Science Center, Basrah University
PO Box 49, Basrah, Al Basrah, Iraq
[2]Physics Department, Science College, Wasit University
Al Kut, Wasit, Iraq
[3]Physics Department, Education College, Baghdad University
Al-Jadriya, Karrada, Baghdad Iraq
Email: adel.mohammed@uobasrah.edu.iq

Abstract

Remote sensing techniques have made it possible to monitor an important parameter of water quality, total dissolved solids (TDS), more appropriately and regularly. The research aims to assess Landsat 8 OLI images' ability to expose TDS on the sea surface in Iraqi marine waters. six band combinations were employed in the correlation analysis between band values and six dissolved solids samples collected during the fieldwork in three sampling stations to determine the amount of total dissolved solids (TDS): st1, st2, and st3 in December 2014 (26,38,36.9) g.L^{-1} and mid-January 2022 (27.4,37.9,37) g.L^{-1}, respectively. Furthermore, two images of the Landsat-8 OLI satellite were captured concurrently with the gathering of samples for TDS detection at the measuring stations. After atmospheric correction and the add the remote sensing indicators, the reflectance of water was extracted from satellite images and utilized to express the spectral characteristics of various TDS concentrations, since the values were (22.64, 38, 32.46) g.L^{-1} in 2014, and (27.5, 36.68, 38) g.L^{-1} in 2022. Correlation coefficient (R2) values of 0.81, 0.96, and Pearson correlation (r) values of 0.90, 0.97 were found among field measurements and spectral data of TDS indicator 2 (SI-2) derived from green, blue, and red bands of Landsat -8 at 2014, 2022 respectively.

Keywords: Iraqi marine water, GIS, Landsat-8, TDS, Spectral indicators

Introduction

Salinity levels and Total dissolved solids (TDS) are closely related concepts because the majority of dissolved solids are made up of the inorganic ions that make up salts, thus, at water bodies, increasing salinity is equivalent to increasing TDS (Ferdous et al., 2019). Among the essential elements in the marine environment is sea surface salinity (SSS), which is crucial in regulating ocean currents and a host of other oceanic phenomena and activities. Knowing, and understanding the SSS distribution can be helpful when researching biochemical and physical processes in the ocean (Chen and Hu, 2017). An increase or decrease in salinity is related to the change in temperature and evaporation rate (Rahi, 2018). Measurements from vessels and buoys are heavily used in conventional SSS monitoring techniques. In reality, frequently these in-situ measurements are expensive and a big time exhaustion, but most significantly, it places a significant constraint on studies of SSS that use spatiotemporal data (Song et al., 2013). These constraints can be overcome by satellite remote sensing if appropriate algorithms are created. Due to real-time observations, and the features of extensive coverage, remote sensing may be a viable substitute for SSS observation. In light of this, many researchers and scientists have given using satellite data to appreciate SSS from space a lot of attention (Marghany et al., 2010). Nevertheless, Despite the importance of salinity, a significant portion of the world's oceans hasn't been measured due to conventional sparse and irregular measurements of salinity (SSS) made by research vessels or using buoys (Zine et al., 2017).

Sampling and laboratory measurements of chemical and physical characteristics are conventional methods of monitoring water quality. So it is time-consuming and costly. A basic technique for studying the environment and water quality, which involves the use of a geographic information system (GIS) in conjunction with remote sensing (RS). These methods make the observation function more efficient in terms of resources and time by providing strong analytical and optical tools for analyzing, characterizing, and modeling natural system

processes (Ferdous *et al.*, 2019). The combining advantages of field data with satellite image analysis to precisely determine water quality have been demonstrated by several authors (Lyon *et al.*, 1988; Härmä *et al.*, 2001; Howari, 2003; Mohamed *et al.*, 2016). As a result, numerous researchers have created mathematical models for evolving RS methods and spectral indicators (Härmä *et al.*, 2001; Dogliotti *et al.*, 2015). These methods comprise analytical and empirical algorithms for creating qualitative or quantitative maps of water (Härmä *et al.*, 2001). To study the water parameters (Minerals, salts, sediments, and other components), it is needful to select a highly reflective spectral package, this is crucial to comprehend the connection between these parameters and their corresponding spectral bands. This research aims to investigate whether it is possible to extract salinity indicators from the Landsat 8 OLI to identify the best equations for forecasting dissolved solids that can be utilized to appreciate salinity depending on their spectral reflectance. The northwestern Arabian Gulf was chosen to be the study and research area because of its great importance in economic, environmental, and geopolitical terms. The study area is located in the far northwest of the head of the Arabian Gulf, so its physical, chemical, and biological properties are mainly affected by the characteristics of the Arabian Gulf. Also, it hosts a wide range of marine ecosystems such as mangrove swamps, seagrass beds, and coral reefs, these ecosystems support marine biodiversity as they constitute shelter, feeding, and nursery areas for a variety of marine organisms (Naser, 2011; Abdel-Jabbar, *et al.,* 2013), of the studies that were

conducted in the study area dealt with certain aspects are estimating evaporation rates (Al-Fartusi and Adel, 2019), as well as a study General characteristics of surface waves (Lafta *et al.,* 2022).

Three stations were selected extending in Iraqi territorial waters distributed as follows (st1, st2, and st3) Figure (1), where (st1) was at the Shatt al-Arab mouth, (st2) was in marine waters, and (st3) at the entrance to Khor Abdullah. At a depth of (10–15 cm) below the water's surface, samples were taken using the samples collector device.

Materials and Methods

To assess and compare levels of salinity in surface waters, satellite data, along with location data, were both used. This study's methodology focuses on examining the connection between spectral indicators and salinity levels in Iraq's marine waters.

Water sampling and satellite imagery

A field visit to the selected measuring stations was conducted in January 2022, where the levels of dissolved solids (TDS) were measured for three samples of surface water at the above sites using electrical conductivity EC meter. Field data collected in December 2014 were taken advantage of by (Abdulnabi, 2016) Table 1, which coincided with obtaining the relevant OLI images in Table 2. Since the simulation case between spectral and field data

Figure 1. The selected locations northwest Arabian Gulf

Table 1. TDS measurements and samples position

Station	Latitude	Longitude	19 Jan. 2022 TDS (g.L⁻¹)	31Dec.2014 TDS (g.L⁻¹)
St1	29º 54' 09"	48º 39' 15"	27.4	26
St2	29º 50' 52"	48º 43' 08"	37.9	38
St3	29º 52' 35"	48º 24' 20"	37	36.9

Table 2. Landsat 8 OLI images characteristics

Images properties	2014	2022
Path and raw of scene	165/39	165/39
Sensor	Operational Land Imager (OLI)	
Bands used in this study	Blue (2), green (3), red (4), and NIR (5)	
Band number	B-2 Visible (0.450–0.51 µm) 30 m B-3 Visible (0.53–0.59 µm) 30 m B-4 Red (0.64–0.67 µm) 30 m B-5 Near-Infrared (0.85–0.88 µm)30 m	
Reflectance-add-band*	- 0.1	
Reflectance-multi band*	2 e-05	
Time Capture	31/12/2014	19/1 /2022
Sun Elevation	32.289°	34.075°

was unavailable, the data gap (from 2014 to 2022) is not included in this study. The slight difference between field sampling time and image capture time (about an hour) has not affected the precision of the analysis outcomes because of change in TDS concentration over several hours is very rare (Abdullah *et al.*, 2017). The study used data from two images of Landsat 8 OLI obtained from the USGS website. The OLI image in World Geodetic System (WGS) 1984 reference and the Universal Transverse Mercator (UTM) coordinate system, allocated of a zone UTM 39. We note the low value of the salt concentration in the first station (st1) compared to the other stations due to dilution because it is at the Shatt al-Arab estuary beginning, thus freshwater reaches it in the case of the ebb.

Image pre-processing and data Set

ArcGIS software v.10.8.1 was used to process RS data. As shown in Figure 2, the image dataset was acquired with four bands 2, 3, 4, and 5 which represent bands blue, green, red, and (near-infrared) NIR bands, respectively. Satellite image brightness values " registered by the sensor as digital number DN values" were transformed to reflectance values utilizing Arc GIS's raster calibration tool. This processing is critical for surface water environmental studies. To extract data from Landsat images, each pixel's digital value was converted to a reflectance value using the equations (1, 2):

$$L_\lambda' = M_L * Q_{cal} + A_L \quad ....(1)$$

Note : L_λ'= TOA reflectance, without correction for solar angle; M_L= BAND- specific multi-rescaling factor =2.0000e-05; A_L= BAND- specific additive rescaling factor = - 0.1, (Table 2); Q_{cal} = Pixel values (DN);

As demonstrated by the following formula, correction of the solar's elevation angle is a crucial component in determining TOA reflectance:

$$L_\lambda = L_\lambda' / \sin(\theta) .... (2)$$

Note : L_λ = TOA reflectance; θ = Solar elevation angle

Multi-spectral salinity Indicator

Equations (1, 2) were used to transform the radiance of the OLI image to TOA spectral reflectance by utilizing its radiance rescaling factors in the metadata file of the OLI data. Necessitates selecting a high-reflectivity spectral package for studying the water parameters because crucial comprehend how these parameters relate to the equivalent spectral bands. Water quality is influenced by minerals, salts, sediments, and other factors. A spectral range with higher reflectance should be used to demonstrate the water element. In water, changes arise due to the depth of the water, the type of bottom, dispersion, and absorption in a column of water (by chlorophyll, suspended sediment, colored dissolved organic matter, etc.) influence spectral signatures measured
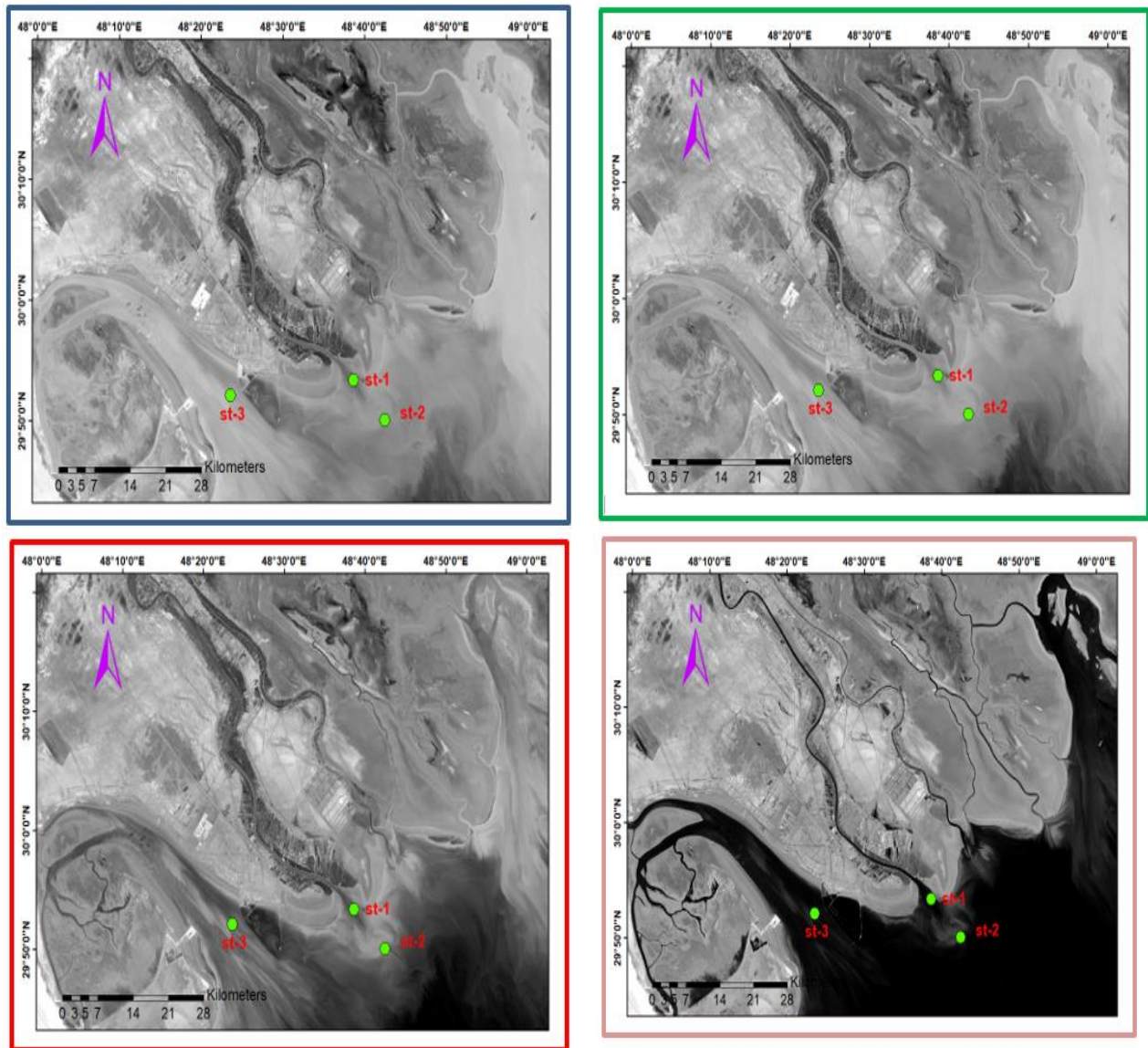
Figure 2. Bands used in the study area: No. 2 (blue), 3 (green), 4 (red), and 5 (NIR).

over water (Howari, 2003). Based on the thorough literature review (Lyon *et al.*, 1988; Abdullah *et al.*, 2017), Selected in this study, many salinity indicators use the VIS visible and NIR infrared bands. The equations used to calculate these indices are displayed in Table 3. The chosen stations' TDS values were calculated from the extracted and configured raster using salinity indicator equations. Equations mentioned in Table 3 were applied to extract the salinity index for two images (2014 and 2022). The output raster's index range values were between (-1 to +1). In the spectral signature value of the water reflectance, the VIS and NIR wavebands (bands 2 and band 5), which are regarded as significant bands for water quality parameters, exhibit a general decrease in reflectance with increasing wavelength.

Regression analysis and correlation

At each measurement station, a satellite image was used to extract spectral band values. To determine the type and power of the relationship between the in-situ TDS measurements and the VIS and NIR spectral bands of the Landsat-8 image, Pearson correlation (r) and simple linear regression (R^2) were computed. This made it possible for us to locate the value at which the spectral and ground data for three stations were highly correlated, which enables us to determine the most accurate indicator.

Results and Discussion

A calculation raster was created using salinity indicator equations after DN values of satellite

images were converted to reflection values. Spectral reflectance values for the three stations are shown in Tables 4, and 5, derived from the salinity raster. Values of (r) and (R2) between the spectral salinity index raster created and the field-measured TDS were acquired to find the strongly correlated values and choose the better indicator.

Shows Table 6, the highest accuracy obtained between the spectral indices with the field data for TDS in the three stations, was for the SI-2 where the (r) value is 0.96 and 0.97 in 2014 and 2022, respectively. These results seem encouraging for using the spectral index to predict salinity, a good second finding was found between TDS and SI-1 with (r) values of 0.75, 0.91 in 2014, and 2022, also SI-3 with (r) values is 0.71, and 0.88 to the same years. To confirm the accuracy of the results for the SI-2, SI-1, and SI-3 indicators, the correlation coefficient (R2) between the two sets of variables (spectral and field data for three stations) was determined using linear regression. As the values were agreeable, Table 6.

The highest salinity indices correlation results from the 2022 OLI image were selected to create three math formulas by linear regression analysis to estimate the salinity of surface water for the study area, as in Figure 3 and Table 7. The findings also demonstrate that salinity indices (SI-2) and (SI-1) are more appropriate. The root mean square of error (RMSE) was calculated between salinity values recorded in the field and the values extracted from Equation No. 2, where found (22.64, 38, 32.46) g.L^{-1} in 2014, and (27.5, 36.68, 38) g.L^{-1} in 2022, respectively in the three measurement stations.

$$\text{RMSE} = \pm\sqrt{\frac{1}{n}\Sigma_{i,j=1}\left(f_i - f_j\right)^2} \quad \text{...............(3)}$$

Where f_i is the value of field measurements and f_j the mean values extracted from Equation No. 2 . It was found that (±1.05) for Jan. 2022, and (±5.5) for December 2014. Equation No. 2 was applied to find the surface salinity values for certain points in the Iraqi territorial waters in January of the year 2022 and

Table 3. Spectral indicators employed in the research. (Morshed *et al.,* 2016)

Indices	Equation
Salinity index 1	$\sqrt{R \ x \ B}$
Salinity index 2	$\sqrt{G \ x \ B}$
Salinity index 3	$\sqrt{R^2 + G^2}$
Salinity index 4	$\sqrt{R^2 + G^2 + NIR^2}$
Salinity index 5	G x R
Salinity index 6	$\sqrt{R^2 \ x \ NIR^2}$

R, red = band 4; B, blue = band 2; G, green = band 3; NIR, near-infrared = band 5

Table 4. Six significant salinity indicators (SI) at three stations on December 31, 2014

Stations	SI-1 $\sqrt{R \ x \ B}$	SI-2 $\sqrt{G \ x \ B}$	SI-3 $\sqrt{R^2 + G^2}$
St-1	0.145085	0.15772	0.140585
St-2	0.16484	0.207506	0.161958
St-3	0.174833	0.189453	0.180133

Table 5. Six significant salinity indicators (SI) at three stations on January 19, 2022

Stations	SI-1 $\sqrt{R \ x \ B}$	SI-2 $\sqrt{G \ x \ B}$	SI-3 $\sqrt{R^2 + G^2}$
St-1	0.145585	0.17365	0.21236
St-2	0.206948	0.203079	0.297926
St-3	0.178133	0.207675	0.251838

Stations	SI-4 $\sqrt{R^2 + G^2 + NIR^2}$	SI-5 G x R	SI-6 $\sqrt{R^2 x \ NIR^2}$
St-1	0.214152	0.021216	0.004803
St-2	0.310573	0.044348	0.01813
St-3	0.253897	0.030274	0.006546

SI = salinity indicator. R, red = band 4; B, blue = band 2; G, green = band3

Table 6. Pearson correlation (r) and coefficient of determination (R^2) for study years

Salinity index (SI)	TDS data 2014		TDS data 2022	
	r	R^2	r	R^2
Salinity index 1	0.91	0.83	0.91	0.84
Salinity index 2	0.96	0.92	0.97	0.96
Salinity index 3	0.84	0.71	0.88	0.78

Table 7. Best TDS Forecasting equations of three stations using salinity index 1, 2, and 3, spectral bands

Landsat 8 OLI image	Forecasting equation	R^2
Salinity indicator 1	Y=174.73(SI-1)+3.2122	0.8439
Salinity indicator 2	Y=309.55(SI-2)-26.181	0.9577
Salinity indicator 3	Y=120.57(SI-3)+3.4893	0.7819
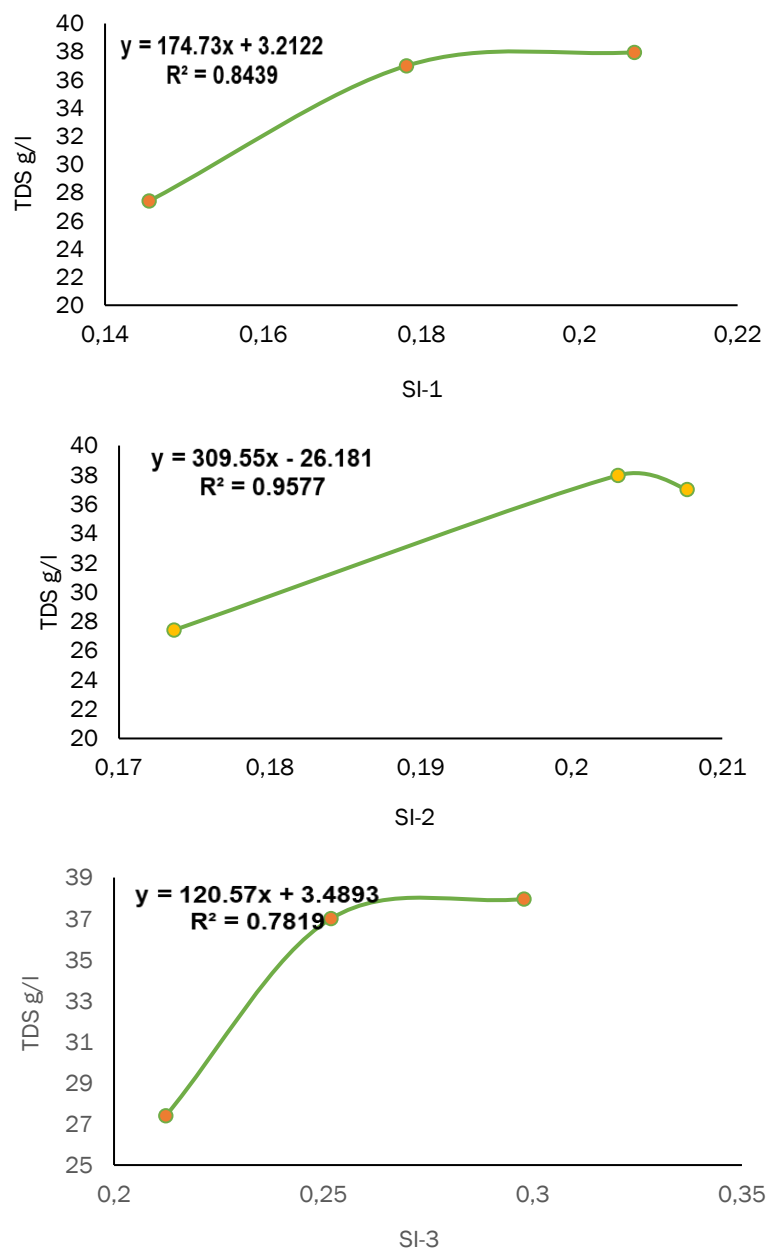
Figure 3. Salinity indicators regression lines SIs (SI-1, SI-2, and SI-3) against TDS values of 2022.

on the same points for December for the year 2014, Figure 4 and Figure 5 represent the surface salinity distribution map for the years 2022 and 2014 in the unit of part per thousand (ppt), respectively.
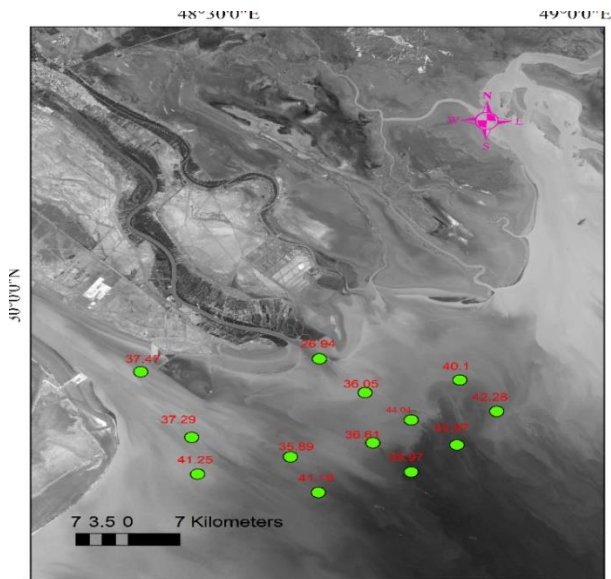
Figure 4. The surface salinity distribution map for the Jan. years 2022
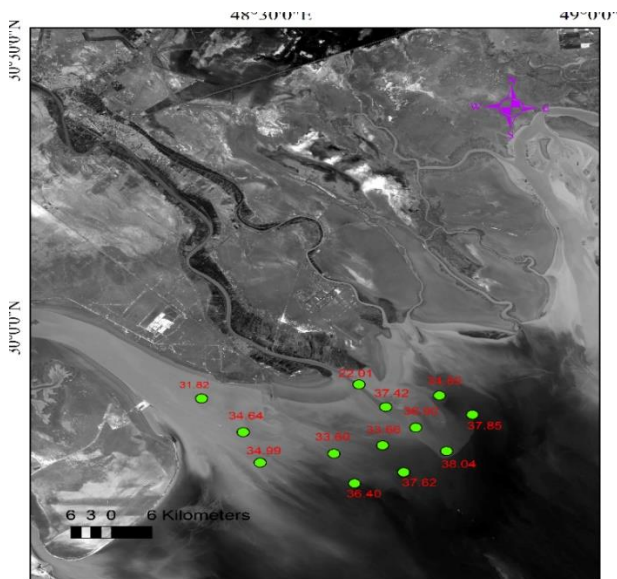
Figure 5. The surface salinity distribution map for the Des. years 2014

The results of this study are consistent with those of another study by (Ferdous *et al*., 2019), which found that different Landsat 8 OLI band compositions can be used to ascertain the salinity level (TDS level) of surface water along Bangladesh's coastline. They affirmed that the Landsat 8 OLI images' blue, green, and red bands could be used to predict the TDS level of coastal surface water, making water monitoring more effective (Ferdous *et al.,*

2019). Another study on water quality at the Al Gharraf stream of Thi-Qar, Iraq, found that there were powerful and positive correlations between water quality parameters and Landsat image reflectance. (Mustafa *et al.,* 2017). According to (Abd *et al.,* 2017), the vegetation indicator of Landsat-8 (OLI) images cannot be used to calculate chemical and physical variables on the water surface.

Conclusions

Nowadays, to develop solutions to resource problems and assess water quality on a large scale, It is necessary to use efficient methods like RS tools. In this paper, the integration of field survey data and Landsat 8 OLI data analysis was demonstrated. To evaluate the salinity of water bodies in the south of Iraq, almost simultaneously, water samples and satellite data were gathered. The coefficient of determination values was utilized to examine the efficacy of the suggested algorithms. Demonstrated current study there was a good correlation between the spectral data of SI-2, although statistical response variability, which was derived utilizing Landsat's green, blue, and red bands, and three field samples, with (r) values of 0.97 and (R^2) values of 0.96 in 2022. Data from the three selected sites underwent regression analysis to confirm associations between TDS and different indicators. Regression values (R^2) of 0.84, 0.96, and 0.78 for SI-1, SI-2, and SI-3, respectively for the OLI image of 2022, indicate a high correlation. According to the findings, SI-2 and SI-1 indices were appropriate for checking the salinity levels in the study zone. The use of spectral index algorithms to supply OLI data provides a strong tool for determining surface water salinity. Three mathematical equations were found to extract the surface salinity values of the water, which are [Y=174.73(SI-1) +3.2122], [Y=309.55(SI-2)-26.181], and [Y=120.57(SI-3) +3.4893], as Equation No. 2 was the best.

Acknowledgement

Reference

Abd, M.H., Mustafa, T.M., Hasson, K.I. & Hussain, M.H. 2017. Using vegetation indices (Ndvi, Rvi, Ipvi, and Dvi) to detect physical and chemical parameters from Landsat-8 (Oli) images when pixel mixing soil, vegetation, and water. *Sch. J. Eng. Tech.,* 5(11): 624–628.

Abdel-Jabbar, N., Baptista, A., Karna, T., Turner, P. & Sen, G. 2013. US Experience Will Advance Gulf Ecosystem Research. *Geo-Informatics in Resource Management and Sustainable Ecosystem: International Symposium, GRMSE 2013, Wuhan, China, November 8-10, 2013, Proceedings, Part II 1,* 399:125–140. https://doi.org/10.1007/978-3-642-41908-9_13

Abdullah, H.S., Mahdi, M.S. & Ibrahim, H.M. 2017. Water quality assessment models for Dokan Lake using Landsat 8 OLI satellite images. *J. Zankoy Sulaimani, Pure, and Applied Sciences*, 19(3-4): 25- 44.

Abdulnabi, Z.A. 2016. Assessment of some toxic elements levels in Iraqi marine water Mesopot. *J. Mar. Sci.*, 31(1): 85–94.

Al-Fartusi, A.J. 2019. Estimation of evaporation rates in the north west Arabian gulf based on sea surface temperature and Meteorological data. *Univ. Thi-Qar J. Sci.,*7(1): 37-40.

Chen, S. & Hu, C. 2017. Estimating sea surface salinity in the northern Gulf of Mexico from satellite ocean color measurements. *Rem. Sens. Environ.*, 201: 115–132.

Dogliotti, A.I., Ruddick, K.G., Nechad, B., Doxaran, D. & Knaeps, E. 2015. A single algorithm to retrieve turbidity from remotely-sensed data in all coastal and estuarine waters. *Rem. Sens. Environ.*, 156: 157–168.

Ferdous, J., Rahman, M.T.U. & Ghosh, S.K. 2019. Detection of total dissolved solids from Landsat 8 OLI image in coastal Bangladesh. *Proc. 3rd Int. Conf. Clim. Change*, 3: 35-44.

Härmä, P., Vepsäläinen, J., Hannonen, T., Pyhälahti, T., Kämäri, J., Kallio, K., Eloheimo, K. & Koponen, S. 2001. Detection of water quality using simulated satellite data and semi-empirical algorithms in Finland. *Sci. Total Environ.,* 268: 107–121.

Howari, F.M. 2003. The use of remote sensing data to extract information from agricultural land with an emphasis on soil salinity. *Soil Research*, 41: 1243–1253. https://doi.org/10.1071/SR03033.

Lafta, A.A. & Al-Fartusi, A.J. 2022. General characteristics of surface waves in Iraq marine water, Northwest of Arabian Gulf . *Arabian J. Geosci.,* 15: p.1598. https://doi.org/10. 1007/s12517-022-10884-y .

Lyon, J.G., Bedford, K.W., Yen, C.C.J., Lee, D.H. & Mark, D.J. 1988. Determinations of suspended sediment concentrations from multiple-day Landsat and AVHRR data. *Rem. Sens. Environ.*, 25: 107–115.

Marghany, M., Hashim, M. & Cracknell, A.P. 2010. Modeling Sea Surface Salinity from MODIS Satellite Data. *Hum. Cent. Comput.,* 6016: 545–556.

Mohamed, M.A., Hussein, A.S. & Lazem, F.L. 2016. Appraisal of some water quality criteria of the Shatt Al-Arab River by applying geographical information system (GIS). *Global J. Biol. Agricult. Health Sci.*, 5: 43–53.

Morshed, M.M., Islam, M.T. & Jamil, R. 2016. Soil salinity detection from satellite image analysis: an integrated approach of salinity indices and field data. *Environ. Monit. Assess.,* 188(2): 119-129. https://doi.org/10.1007/s10661-015-5045-x

Mustafa, T.M., Hasson, K.I., Hussain, H.M. & Abd, M.H. 2017. Using water indices (NDWI, MNDWI, NDMI, WRI, and AWEI) to detect physical and chemical parameters by applying remote sensing and GIS techniques. *Int. J. Res. Granthaalayah*, (5): 117–128. https://doi.org /10.5281/zenodo.1040209.

Naser, H. 2011. Human impacts on marine biodiversity: Macrobenthos in Bahrain, Arabian Gulf. In The Importance of Biological Interactions in the Study of Biodiversity; Lopez-Pujol, J., Ed.; In Tech Publishing: Rijeka, Croatia: p.109–126.

Rahi, K.A. 2018. Salinity management in the Shatt Al-Arab River. *Int. J. Eng. Technol.,* 7(4.20): 128–133.

Song, Q.; Zhang, J.; Cui, T. & Bao, Y. 2013. Retrieval of sea surface salinity with MERIS and MODIS data in the Bohai Sea. *Remote Sens. Environ.,* 136: 117–125.

Zine, S., Boutin, J,. Waldteufel. P., Vergely, J.L., Pellarin. T. & Lazure P. 2017. Issues about retrieving sea surface salinity in coastal areas from SMOS data. *IEEE Trans. Geosci. Remote Sens.*, 45(7): 2061-20